**ORIGINAL ARTICLE**

CrossMark

# Effects of stability of PEGylated micelles on the accelerated blood clearance phenomenon

Yuqing Su[1] · Mengyang Liu[1] · Yan Xiong[1] · Junqiang Ding[1] · Xinrong Liu[1] · Yanzhi Song[1] · Yihui Deng[1] (iD)

## Abstract

Accelerated blood clearance (ABC) is a phenomenon where the blood clearance rate of the carrier system is substantially raised. It can be induced by repetitive injections of polyethylene glycol (PEG) (molecular weight 2000)-modified micelles (PM2000). To determine whether the PEG chain length and PEGylated micelle injection dose can have an effect on the ABC phenomenon, micelles were modified with PEGs of varying molecular weights; PEGs with molecular weights of 350, 550, 2000, 5000, 10,000, and 20,000 were used to generate the PEGylated micelles PM350, PM550, PM2000, PM10000, and PM20000, respectively. One special carrier, MCT-PM2000, was prepared with the original PM2000 formulation but also included extra medium-chain triglycerides. Our experimental results showed that PM2000 and PM5000 exhibit superior storage stability compared to that of PM350, PM550, PM10000, and PM20000. MCT-PM2000 demonstrated stronger dilution stability than PM2000. As expected, PM2000 and PM5000 induced the strongest enhancement in blood elimination rate compared to that of PM350, PM550, PM10000, and PM20000; MCT-PM2000 exhibited more intense ABC phenomenon compared to that of PM2000. In addition, induction of the ABC phenomenon by PM2000 and MCT-PM2000 was augmented when the injection dose was increased from 0.05 to 5 μmol phospholipid·kg$^{-1}$. Based on our findings, we suggest that there is a positive linear relationship between stability of PEG-modified micelles and susceptibility to the ABC phenomenon. The results may be valuable for designing PEGylated micelles for multiple drug therapy.

**Keywords** Accelerated blood clearance · PEGylated micelles · PEG chain length · Lipid dose · Anti- · PEG IgM

## Abbreviations

| | |
|---|---|
| 5%Glu | 5% (*m/v*) glucose for injection |
| HLB | the hydrophilic lipophilic balance |
| CMC | critical micellization concentration; |
| AUC | area under the curve |
| MRT | mean residence time |
| DSPE-PEGx | 1,2-distearoyl-sn-glycero-3-phosphoethanolamine-*n*-[methoxy(polyethylene glycol)-x] (x = 350, 550, 2000, 5000, 10,000 and 20,000) |
| MCT | medium-chain triglycerides |
| PM | PEGylated micelles |
| PE | PEGylated emulsion |
| PMy (y = 350, 550, 2000, 5000, 10,000 and 20,000) | micelles composed of DSPE-PEGx, x = 350, 550, 2000, 5000, 10,000 and 20,000, respectively |
| MCT-PM2000 | micelles composed of DSPE-PEG$_{2000}$ with MCT in the inner core (Weight of DSPE-PEG$_{2000}$ weight of MCT, 14: 1, *w/w*) |
| PMy-PE | PMy were pre-administered into rats, and PE were injected 7 days later |
| PM2000 (zCMC)-PE | PM2000 were pre-administered into rats at a dose of z-fold of the CMC of DSPE-PEG$_{2000}$, and PE were injected 7 days later |
| MCT-PM2000 (zCMC)-PE | MCT-PM2000 were pre-administered into rats at a dose of z-fold of the |

✉ Yanzhi Song
songyanzhi@syphu.edu.cn

✉ Yihui Deng
dengyihui@syphu.edu.cn

[1] School of Pharmacy, Shenyang Pharmaceutical University, 26 Huatuo Road, Benxi 117004, People's Republic of China

CMC of DSPE-PEG$_{2000}$, and PE were injected 7 days later

CMC2000  the CMC value of the DSPE-PEG$_{2000}$
EE  encapsulation efficiency

## Introduction

The accelerated blood clearance (ABC) phenomenon occurs during repetitive administration of PEGylated nanocarriers or PEGylated proteins into animals, where rapid blood clearance of subsequent PEGylated nanocarriers occur, along with their accumulation in the liver and spleen [1–7]. The ABC phenomenon is of clinical concern, as it decreases the therapeutic efficacy of an encapsulated drug, and may cause adverse effects [8, 9]. Polymeric micelles, a type of nanocarrier for drug delivery systems (DDS), are formed from block copolymers, and are composed of an inner core (hydrophobic, cationic or anionic) and a hydrophilic outer shell [10]. The hydrophilic shell is usually made up of PEG, as PEG is generally regarded to be safe by the Food and Drug Administration. Currently, a number of PEGylated micelles with encapsulated anticancer drugs are undergoing clinical trials and exhibit important application values [11–13]. Unfortunately, PEGylated micelles can induce the ABC phenomenon; micelles size [6], the hydrophobic inner core [14, 15], and micelle components [16] can all influence the extent of the ABC phenomenon. Therefore, it is necessary to investigate other factors that play a role on the ABC phenomenon.

Up to now, many factors have been reported to be associated with the ABC phenomenon, including the injection dose, the physicochemical properties [17] of PEGylated carriers, and the time interval between administrations [18, 19]. The effect of injection dose on the ABC phenomenon is highly dependent on the properties of the first dose, such as the type of nanocarrier, and whether the nanocarrier possesses a PEG outer shell. For example, intravenously injected PEGylated liposomes at a dose of 0.001 μmol phospholipid·kg$^{-1}$ can induce the strongest ABC phenomenon [18]. However, conventional liposomes (liposomes without PEG outer shell) are unable to induce the ABC phenomenon at a dose of 0.001 μmol phospholipid·kg$^{-1}$ [18]. PEGylated solid lipid nanoparticles induced the strongest ABC phenomenon at a dose of 5 μmol phospholipid·kg$^{-1}$ [3]. In addition, only DSPE-PEG$_{2000}$ and DSPE-PEG$_{5000}$ were used to study the effect of PEG chain length on PEGylated liposome-induced ABC phenomenon [18]; results indicated that the ABC phenomenon induced by PEGylated liposomes cannot be affected by DSPE-PEG$_{2000}$ or DSPE-PEG$_{5000}$. However, to date, no systematic study has been conducted on the effect of PEG length and lipid dose on the ABC phenomenon in PEGylated micelles.

In the present study, we investigated the storage stability of PM350, PM550, PM2000, PM10000, and PM20000 on the dilution stability of PM2000 and MCT-PM2000. The extent to which the ABC phenomenon is induced by these PEGylated micelles was studied in detail. Furthermore, the effect of stability, lipid dose, and PEG chain length of these PEGylated micelles were discussed. Our results strongly suggested that susceptibility to the ABC phenomenon is positively correlated with stability of the PM. In addition, PEG chain length and injection dose can also significantly affect the extent of the ABC phenomenon. When HLB and CMC values of DSPE-PEGx ($x = 350, 550, 2000, 5000, 10,000,$ and 20,000) were measured, we found that CMC and HLB values of unimers do not exert any effect on the ABC phenomenon.

## Materials and methods

### Materials and animals

DSPE-PEGx ($x = 350, 550, 2000, 5000, 10,000$ and 20,000, Genzyme, USA), MCT (Beiya Medicated Oil, China), egg phosphatidylcholine (E80, Lipoid GmbH, Germany), dialkylcarbocyanines (DiR, AAT Bioquest, USA), Sephadex G-50 (Sigma-Aldrich, USA), Tris (Sigma-Aldrich, USA), bovine serum albumin (BSA, Biosharp, Korea), rabbit anti-rat IgM (Beijing Biosynthesis Biotechnology, China), and O-phenylenediamine (Sigma-Aldrich, USA).

Male Wistar rats (180–200 g) were obtained from the experimental animal center of Shenyang Pharmaceutical University, China. Animals were maintained under conventional conditions and were fed standard laboratory chow and water ad libitum. All animal care procedures and experiments were carried out according to the guidelines of the animal welfare committee of Shenyang Pharmaceutical University (NIH publication #85–23, revised in 1985).

### HLB value of DSPE-PEGx

HLB values were calculated according to Griffin's formula [20]:

$$HLB = 20 \, m_w / M_w$$

where $m_w$ is the molecular weight of PEGx ($x = 350, 550, 2000, 5000, 10,000,$ and 20,000) and $M_w$ is the molecular weight of the whole molecule of DSPE-PEGx ($x = 350, 550, 2000, 5000, 10,000,$ and 20,000).

### CMC value of DSPE-PEGx

The pyrene fluorescence method [21] was used for CMC determination of DSPE-PEGx ($x = 350, 550, 2000, 5000,$

68

Drug Deliv. and Transl. Res. (2019) 9:66–75

10,000, and 20,000). A solution of pyrene was prepared in methanol at a concentration of $10^{-5}$ M and was then transferred into a series of clean penicillin bottles (0.1 mL/bottle); solutions were dried under nitrogen. DSPE-PEGx with various molecular weights was added into these penicillin bottles, followed by 10 mL pure water; the ultrasound technique was carried out in a 60 °C water bath. Following overnight incubation, aqueous solutions with $10^{-7}$ M pyrene were obtained. The concentrations of DSPE-PEGx in the solutions were $10^{-9}$, $10^{-8}$, $10^{-7}$, $10^{-6}$, $10^{-5}$, $10^{-4}$, $10^{-3}$, and $10^{-2}$ M. The control group was prepared by following the same steps described above without DSPE-PEGx. The concentration of solubilized pyrene in micellar phase was determined spectrofluorometrically at excitation and emission wavelengths of 300–350 nm and 390 nm, respectively.

## Preparation of PEGylated nanocarriers

### Preparation of PEGylated micelles

PEGylated micelles were prepared using a self-assembly method [22]. DSPE-PEG350 (5.76 mg), DSPE-PEG550 (6.76 mg), DSPE-PEG2000 (14.00 mg), DSPE-PEG5000 (29.00 mg), DSPE-PEG10000 (54.00 mg), and DSPE-PEG20000 (104.00 mg) were dissolved in 0.2 mL absolute ethanol or 3 mg MCT at 55 °C to form a homogeneous phase. Sterile water was then added to achieve a clear, injectable micelle solution (3 mL). Each mixture was sonicated in an ice bath using an ultrasonic cell pulverizer (JY92-II, Ningbo Scientz Biotechnology Co., Ltd., Zhejiang, People's Republic of China) at 200 W. A submicron particle sizer (Nicomp 380™, Particle Sizing Systems, Inc., Santa Barbara, CA, USA) was used to confirm that the final particle size in each group was approximately 20 nm. The final solution was filtered through a polycarbonate membrane with a pore size of 0.22 μm.

### Preparation of PEGylated nanoemulsions

The oil phase containing DiR: MCT: E80: DSPE-PEG2000 (3.21:72.89:17.05: 6.85, *w/w*) was dissolved at 55 °C. Under the same temperature, sterile water was injected into the oil phase (oil phase: water phase is 1:33.8, *w/w*), and the mixture was stirred for 10 min at 55 °C in water bath to obtain primary emulsions [23]. Final emulsions were obtained using a M-110L Microfluidizer Processor (Microfluidics Company, USA) at 14,000 psi for 14 cycles (primary emulsions, 30 mL). The emulsions were extruded through polycarbonate membranes with a pore size of 0.22 μm. PEGylated nanoemulsions containing DiR was referred to as PE (test dose).

## Determination of PM stability

To examine the storage stability of PM, changes in appearance were observed after incubating PM350, PM550, PM2000, PM5000, PM10000, and PM20000 at 25 °C for 60 days under nitrogen protection. In order to study PM dilution stability, PM2000 and MCT-PM2000 were diluted to 12% of CMC2000, and particle size changes were monitored by the Nicomp 380 HPL submicron particle analyzer.

## The ABC phenomenon of PM

For the first injections, 45 rats (180–200 g) were divided into 15 groups ($n = 3$). The control group received 5% Glu intravenously. One group was administrated DSPE-PEG2000 molecule (0.005 μmol phospholipid·kg$^{-1}$). Six groups were administered PM350, PE550, PM2000, PM5000, PM10000, and PM20000 (5 μmol phospholipid·kg$^{-1}$) intravenously. In three groups, PM2000 was administered at 0.05, 1, and 5 μmol phospholipid·kg$^{-1}$ by the intravenous route. In the remaining groups, MCT-PM2000 was intravenously administrated at doses of 0.05, 1, and 5 μmol phospholipid·kg$^{-1}$. Seven days later, all groups were given 5 μmol phospholipid·kg$^{-1}$ PE (test dose) through the caudal vein. Following this, blood samples (0.5 mL) were collected at predetermined post-injection time points (1 min, 15 min, 30 min, 1 h, 4 h, and 8 h) through the retro-orbital sinus; blood was centrifuged at 4500 rpm for 10 min to obtain the plasma. Plasma samples containing DiR were processed as follows: 100 μL plasma samples were mixed with ethyl alcohol (900 μL); the entire mixture was vortexed for 5 min and centrifuged at 10,000 rpm for 10 min; the supernatant (600 μL) was centrifuged at 10,000 rpm for another 10 min; the final supernatant (200 μL) was added into 96-well plates and analyzed using a microplate reader (Bio-Rad Laboratories, Hertfordshire, UK). The detection wavelengths were 750 nm (excitation) and 790 nm (emission). The pharmacokinetic values, AUC (0-∞), and Cmax were measured using the DAS pharmacokinetic software (2.0 version).

## Statistical analysis

Data were presented as means ± standard deviation. All the experiments were repeated for at least three times with three replicates. Statistical comparisons were performed using two-tailed unpaired Student's *t* tests or ANOVAs with the SPSS 16.0 software (IBM, New York, USA). Statistical significance was set at *$p < 0.05$, **$p < 0.01$, and ***$p < 0.001$.

Drug Deliv. and Transl. Res. (2019) 9:66–75

69

# Results

## Characterization of the DSPE-PEGx

For CMC determination, due to its functionality, versatility, and easy application, the pyrene method was chosen. As shown in Table 1, the CMC values of DSPE-PEGx ($x$ = 350, 550, 2000, 5000, 10,000, and 20,000) were $0.98 \times 10^{-5}$, $1.05 \times 10^{-5}$, $1.38 \times 10^{-5}$, $2.29 \times 10^{-5}$, $2.63 \times 10^{-5}$, and $4.90 \times 10^{-5}$ M. It was clear that CMC values were slightly increased with increased proportion of the hydrophilic component in the polymer. The results were consistent with the observation that the nature of soluble hydrophilic blocks is only slightly dependent on micellization [21, 24]. In addition, the HLB values of DSPE-PEGx ($x$ = 350, 550, 2000, 5000, 10,000 and 20,000) were 5.44, 7.81, 14.11, 17.41, 18.49, and 19.21. The results suggested that CMC values are well associated with HLB values.

## Characterization of PEGylated carriers

As reported, repeated injections of polymeric micelles can promote the ABC phenomenon in a size-dependent manner [6]. Hence, it is necessary to control the particle size in this study. To keep the PM sizes at approximately 20 nm, PMs were prepared with an ultrasonic cell pulverizer; power was closely monitored. In addition, diameters/Zeta potentials of PMs were characterized; detailed experimental methods are described in the Electronic Supplementary Information. As shown in Table 2, the mean hydrodynamic diameters of PMs were between $16.29 \pm 3.32$ and $23.28 \pm 3.84$ nm; these particle sizes ensured formation of polymeric micelles. In addition, the hydration shell formed by PEG and the Zeta potential were between $-11.17 \pm 0.62$ mV and $-49.00 \pm 2.36$ mV, which showed that PM can maintain stability against aggregation.

## Characterization of the test dose (PE)

Physical properties of PE, such as diameters, Zeta potentials, DiR cumulative release, and EE (encapsulation efficiency) were characterized. Detailed experiment methods are

**Table 1** Properties of polymers used in micelles preparation

|  | MW of PEG (g·mol$^{-1}$) | HLB | CMC(M) |
|---|---|---|---|
| DSPE-PEG$_{350}$ | 308 | 5.44 | $0.98 \times 10^{-5}$ |
| DSPE-PEG$_{550}$ | 528 | 7.81 | $1.05 \times 10^{-5}$ |
| DSPE-PEG$_{2000}$ | 1980 | 14.11 | $1.38 \times 10^{-5}$ |
| DSPE-PEG$_{5000}$ | 4972 | 17.14 | $2.29 \times 10^{-5}$ |
| DSPE-PEG$_{10000}$ | 9988 | 18.48 | $2.63 \times 10^{-5}$ |
| DSPE-PEG$_{20000}$ | 19,976 | 19.21 | $4.90 \times 10^{-5}$ |

**Table 2** The mean particle size and Zeta potential of PMy and PE

|  | Size (nm) | Zeta potential (mV) |
|---|---|---|
| PM350 | $19.22 \pm 6.24$ | $-41.78 \pm 1.51$ |
| PM550 | $20.04 \pm 8.09$ | $-30.79 \pm 0.40$ |
| PM2000 | $16.95 \pm 2.24$ | $-49.00 \pm 2.36$ |
| PM5000 | $15.81 \pm 1.11$ | $-30.53 \pm 1.55$ |
| PM10000 | $17.27 \pm 3.89$ | $-14.64 \pm 0.77$ |
| PM20000 | $16.29 \pm 3.32$ | $-11.17 \pm 0.62$ |
| MCT-PM2000 | $23.28 \pm 3.84$ | $-47.26 \pm 0.41$ |
| PE | $147.3 \pm 4.20$ | $-58.21 \pm 2.85$ |

described in the Electronic Supplementary Information. In this study, the mean diameter of PE-loaded DiR was $147.3 \pm 4.2$ nm (Table 2). The Zeta potential has an important effect on the stability of the colloid dispersion system. As shown in the Table 2, PE is negatively charged, with a Zeta potential of approximately $-58.21 \pm 2.85$ mV. The electrostatic repulsion between the nanoemulsion and the PEG hydration shell aids in the maintenance of a sterically stable state. The stability of the nanoemulsions was indirectly demonstrated via drug release (Fig. 1). The in vitro DiR release kinetics of PE was found to obey the Ritger-Peppas equation ($R^2 = 0.9818$); less than 7% of DiR was released from PE in 48 h. The mean value of the EE (%) of DiR in PE was 98.9%. Moreover, our previous work showed that DiR is optimal for studying the ABC phenomenon due to its near-infrared fluorescence, high-sensitivity, and convenient analytical detection [25]. Hence, PE was used as a scientific test dose to measure the extent of the ABC phenomenon induced by PEGylated micelles in the current study.

## Stability studies

### Storage stability of PM at room temperature

Ordinary polymeric micelles are in a dynamic state and present only temporal stability [26]. To examine the stability of PM, we incubated PM at 25 °C for 60 days under nitrogen
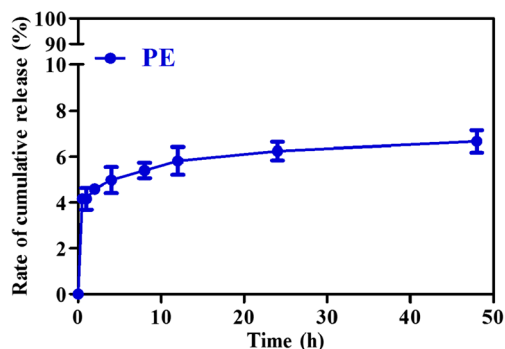


**Fig. 1** The rate of DiR cumulative releases from PE in 48 h in vitro. The release kinetics follows the Ritger-Peppas equation. Data are shown as means ± standard, $n = 3$

protection. Particle aggregation of PM350, PM550, PM10000, and PM20000 was observed; however, PM2000 and PM5000 were still transparent following the incubation period (Fig. 2). Particle stability has a tendency to first increase, and then decrease; the CMC and HLB values increased with greater proportion of the hydrophilic component in the polymer (Table 1). The most stable PMs were PM2000 and PM5000.

### The dilution stability of PM

The threshold concentration for micelle formation is known as CMC. To study the residence time of micelle clusters below the CMC, PM2000 and MCT-PM2000 concentrations were diluted to 12% of CMC2000. As shown in Figs. 3, 80 min following PM2000 dilution, PM2000 dissociated, and particle size decreased from $16.95 \pm 2.24$ to $0.7637 \pm 0.1164$ nm. However, MCT-PM2000 was more stable than PM2000. Even 24 h after MCT-PM2000 dilution, the size of MCT-PM2000 was enlarged, but with no micelle dissociation.

### The ABC phenomenon induced by PM in different hydrophilic chain length

In order to determine whether PEG chain length of the first-dose PM affects induction of the ABC phenomenon, rats were treated with 5 μmol phospholipid·kg$^{-1}$ of PM350, PM550, PM2000, PM5000, PM10000, and PM20000. Seven days later, the concentration-time curves of the test dose (PE) were determined (Fig. 4a). The pharmacokinetic values, the AUC$_{(0-\infty)}$, and the MRT$_{(0-8h)}$ were measured by the DAS pharmacokinetic software. Both PM2000 and PM5000 showed enhanced blood elimination rate compared to that of PM350, PM550, PM10000, and PM20000 (Fig. 4a). The AUC$_{(0-8h)}$ values of PM2000-PE and PM5000-PE groups were $6669.03 \pm 441.234$ and $5764.58 \pm 568.111$, respectively ($p = 0.12$), and the MRT$_{(0-8h)}$ values of PM2000-PE and PM5000-PE were $84.028 \pm 12.10$ and $88.219 \pm 10.27$, respectively ($p = 0.68$) (Table 3). In this study, the ABC indices were determined by the following equation: ABC index = AUC$_{(0-8h)}$ mean value



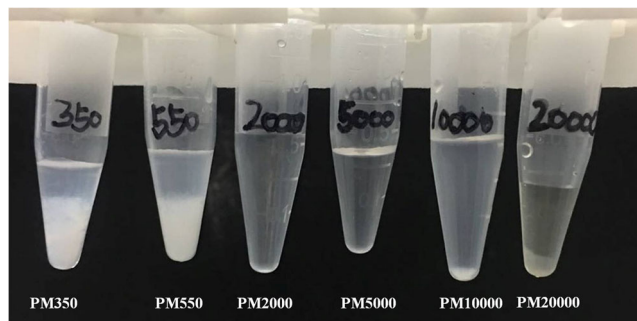**Fig. 2** The particle aggregation of PMy after storing for 60 days at room temperature ($y$ = 350,550, 2000, 5000, 10,000, and 20,000)

of the second injection/AUC$_{(0-8h)}$ mean value of the first injection. A higher index represents a weaker ABC phenomenon. As demonstrated by Fig. 4b, as the ratio of the hydrophilic component increases in the polymer, the ABC phenomenon shows greater tendency to first increase, then decrease. The most stable PMs, PM2000 and PM5000, induced the strongest ABC phenomenon. Therefore, we propose that the extent of the ABC phenomenon induced by micelles can be inferred by observing the storage stability of these micelles.

### The ABC phenomenon induced by PM2000 at different injection doses

To study the effect of the lipid dose on the ABC phenomenon, PM2000 (0.05, 1.0, and 5.0 μmol phospholipid·kg$^{-1}$) and the DSPE-PEG$_{2000}$ molecule (0.005 μmol phospholipid·kg$^{-1}$) were given as the first injection dose, while 5 μmol phospholipid·kg$^{-1}$ PE was given as the second dose. For the control group, 5% Glu was used as the first dose. When micelles are diluted below the CMC, micelles will dissociate into molecules. For rats, 1 kg body weight contains 30 mL blood plasma. Table 1 shows that the CMC value of DSPE-PEG$_{2000}$ is $1.38 \times 10^{-5}$ M. Therefore, when 0.05, 1.0, and 5.0 μmol phospholipid·kg$^{-1}$ of PM were injected into the circulation, the concentration of PM2000 decreased to 0.017, 0.033, and 0.17 μmol phospholipid·mL$^{-1}$, respectively. The values 0.017, 0.033, and 0.17 μmol phospholipid·mL$^{-1}$ were 0.12-, 2.4-, and 12.1-fold of CMC2000, respectively.

As shown in Fig. 5, the first dose of DSPE-PEG$_{2000}$ molecule (0.005 μmol phospholipid·kg$^{-1}$) was unable to induce the ABC phenomenon in PE (ABC index, 0.94). When DSPE-PEG$_{2000}$ molecule self-assembled into PM2000, the ABC phenomenon occurred in PE. The extent of the ABC phenomenon by PM2000 increased when the first dose was increased from 0.05 to 5 μmol phospholipid·kg$^{-1}$ (the ABC index, 0.47, 0.4, and 0.39 respectively). As shown by Fig. 3a, b, when PM2000 concentration was diluted to 12% of CMC2000, the micelles dissociated into individual molecules ($0.7637 \pm 0.1164$ nm) in 80 min. However, following injection of 0.05 μmol phospholipid·mL$^{-1}$ PM2000 into the circulation, the ABC phenomenon can be induced (Fig. 5). Therefore, if the first injection is not DSPE-PEG$_{2000}$, injected micelles can only be stable for at most 80 min in the circulation, and the ABC phenomenon can be induced.

### The ABC phenomenon induced by MCT-PM2000 at different injection dose

We also studied the effect of PM2000 dilution stability on the ABC phenomenon. The MCT-PM2000, which was of PM2000 and MCT (1 mg·mL$^{-1}$), was first injected into rats at doses of 0.05, 1.0, and 5.0 μmol phospholipid·kg$^{-1}$. The
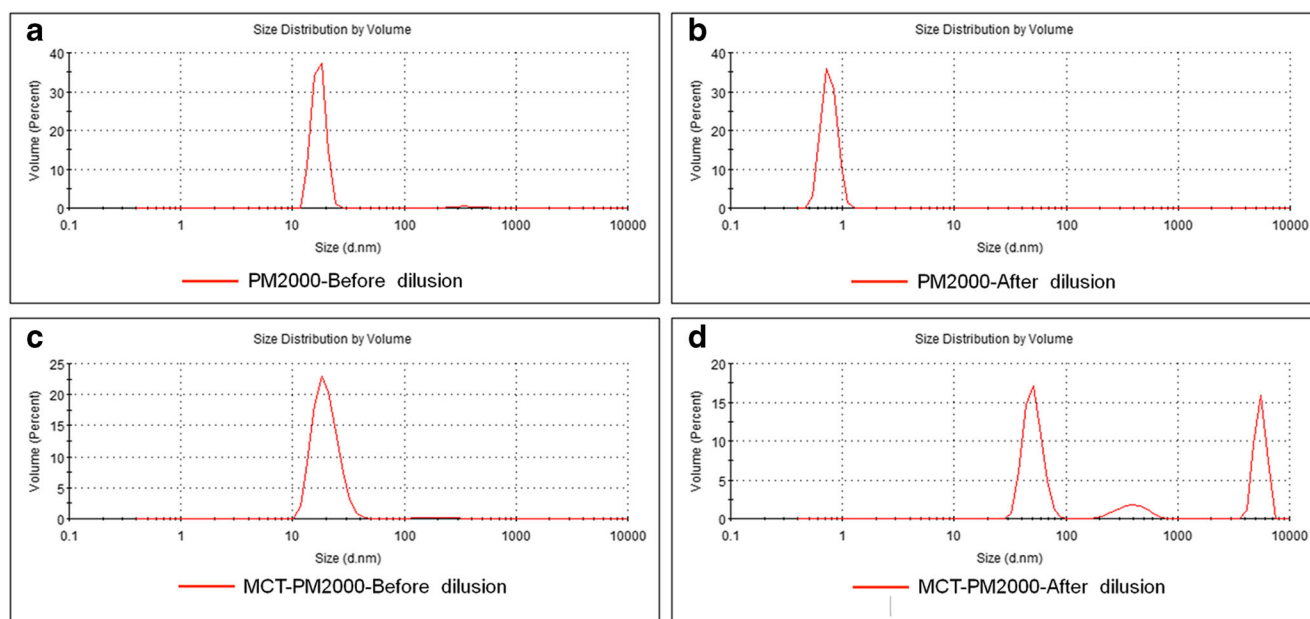
**Fig. 3** The particle size distribution of PM2000 and MCT-PM2000. **a** The particle size distribution of PM2000 before dilution. **b** The particle size distribution of PM2000 in 80 min after dilution to 12% of the CMC value of DSPE-PEG$_{2000}$ (CMC2000). **c** The particle size distribution of MCT-PM2000 before dilution. **d** The particle size distribution of MCT-PM2000 in 24 h after dilution to 12% of CMC2000

control group was pretreated with 5% Glu. Seven days later, DiR-labeled PE was administered to determine susceptibility to the ABC phenomenon. By increasing the first dose of MCT-PM2000 from 0.05 to 5 μmol phospholipid·kg$^{-1}$, induction of the ABC phenomenon was increased (AUC$_{(0-8h)}$, $144.862 \pm 26.129$, $1820.897 \pm 145.182$, $3167.709 \pm 225.941$; % injection dose·L$^{-1}$·min). Moreover, as compared with that of PM2000 (ABC index, 0.47), the ABC phenomenon of MCT-PM2000 (ABC index, 0.18) exhibited significant enhancement. When the concentration of MCT-PM2000 was diluted to 12% of CMC2000, micelles remained intact 24 h later (Fig. 3c, d). As a result, by increasing the interfacial tension between solvophobic block and the solvent, dilution stability is increased, and the ABC phenomenon is more prominent (Fig. 6).

## The anti-PEG IgM induced by PM

It has been demonstrated that the anti-PEG IgM secreted by splenic B cells is associated with the ABC phenomenon [27–29]. Therefore, we investigated whether PMy ($y = 350$, 550, 2000, 5000, 10,000, and 20,000) at 5 μmol phospholipid·kg$^{-1}$, PM2000, or MCT-PM2000 at 0.05 μmol phospholipid·kg$^{-1}$ can induce anti-PEG IgM production in rats. Seven days after the first injection, serum anti-PEG IgM was measured by the ELISA. Detailed experiment methods are described in the Electronic Supplementary Information. As shown in Fig. 7, with increased PEG chain length, secretion of anti-PEG IgM was initially elevated, followed by a decrease. MCT-PM2000 with better dilution stability can induce greater secretion of anti-PEG IgM than PM2000.
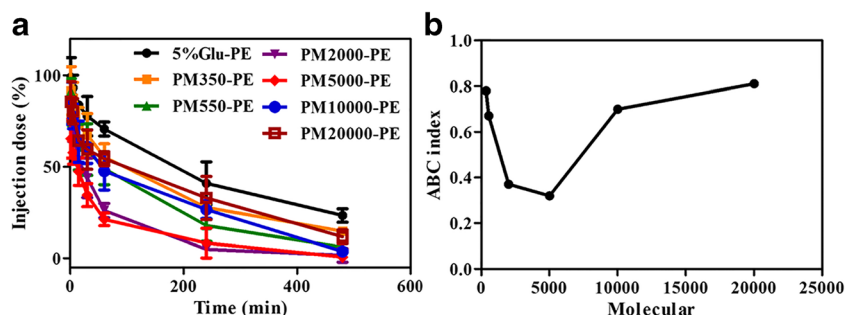


**Fig. 4** The rats were pretreated with 5 μmol phospholipid·kg$^{-1}$ of PM350, PM550, PM2000, PM5000, PM10000, and PM20000, and 7 days later, each group was intravenously injected with 5 μmol phospholipid·kg$^{-1}$ of PE. **a** The concentration-time curve of the second dose of PE. **b** The ABC index of PM350, PM550, PM2000, PM5000, PM10000, and PM20000 group. Data are shown as means ± standard, $n = 3$

72

Drug Deliv. and Transl. Res. (2019) 9:66–75

**Table 3** The pharmacokinetic parameter and the ABC index of the second administration of PE

|  | $AUC_{(0\text{-}8h)}$ (%Injection dose·L$^{-1}$·min) | $MRT_{(0\text{-}8h)}$ (min) | ABC Index |
|---|---|---|---|
| 5%Glu-PE | 17,804.208 ± 3384.292 | 142.033 ± 16.32 | – |
| PM350-PE | 14,008.316 ± 1887.275 | 125.982 ± 22.27 | 0.79 |
| PM550-PE | 11,961.856 ± 1579.199 | 111.906 ± 13.33 | 0.67 |
| PM2000-PE | 6669.03 ± 441.234 | 84.028 ± 12.10 | 0.37 |
| PM5000-PE | 5764.58 ± 568.111 | 88.219 ± 10.27 | 0.32 |
| PM10000-PE | 12,525.925 ± 2133.187 | 109.31 ± 12.08 | 0.70 |
| PM20000-PE | 14,486.186 ± 2750.369 | 128.253 ± 24.17 | 0.81 |
| PM(12.1CMC)-PE | 6991.527 ± 472.930 | 83.804 ± 14.11 | 0.39 |
| PM(2.4CMC)-PE | 7134.429 ± 625.739 | 98.194 ± 10.81 | 0.40 |
| PM(0.12CMC)-PE | 8441.569 ± 332.662 | 118.74 ± 15.38 | 0.47 |
| DSPE-PEG$_{2000}$ molecule-PE | 16,755.751 ± 2185.955 | 131.085 ± 11.21 | 0.94 |
| MCT-PM(12.1CMC)-PE | 144.862 ± 26.129 | 70.012 ± 9.14 | 0.0081 |
| MCT-PM(2.4CMC)-PE | 1820.897 ± 145.182 | 84.006 ± 11.09 | 0.10 |
| MCT-PM(0.12CMC)-PE | 3167.709 ± 225.941 | 98.194 ± 14.45 | 0.18 |

## Discussion

The general accepted mechanism for micelle formation includes two steps. The first step consists of rapid nucleation of unimers, which grow until an optimal size is reached. A thermodynamic equilibrium in micelle quantity is then achieved either by exchanging unimers or by fusion/fission [30]. In many cases, it is difficult to reach thermodynamic equilibrium. The interfacial tension between the solvophobic block and the solvent determines the energy barrier that the hydrophilic chains must overcome. In this study, the formation of PM350, PM550, PM2000, PM5000, PM10000, and PM20000 also underwent the above two steps. Micelle unimers, DSPE-PEGx (x = 350, 550, 2000, 5000, 10,000, and 20,000), have the same solvophobic block and provide

similar energy barriers. The PEG chain is hydrophilic and is essential for micelle formation. The PEG chain can overcome the energy barrier and lead the unimers to form micelles. As demonstrated by our results, after 60 days of incubation at 25 °C, PM350, PM550, PM2000, PM5000, PM10000, and PM20000 exhibited different characteristics. We found precipitates in the PM350, PM550, PM10000, and PM20000 groups. DSPE-PEG350 and DSPE-PEG550 rapidly associate via nucleation and growth, but the energy barrier cannot be easily broken by short PEG chains. Therefore, PM350 and PM550 prefer to aggregate and form precipitates. DSPE-PEG2000 and DSPE-PEG5000 can provide the proper PEG chains, and therefore remain in a transparent state after 60 days. However, elongation of PEG chain increases the likelihood of intertwined PEG chains between micelles. As a
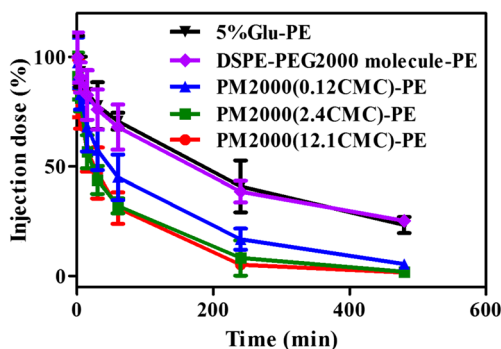


**Fig. 5** The effects of lipid dose of PM2000 on the ABC phenomenon in rats. The rats were pretreated with the DSPE-PEG2000 molecule (0.005 μmol phospholipid·kg$^{-1}$) and PM2000 (0.05, 1.0, and 5.0 μmol phospholipid·kg$^{-1}$, and 7 days later, each group was intravenously injected with 5 μmol phospholipid·kg$^{-1}$ of PE. In addition, after the intravenous injection of PM2000 into circulation at doses of 0.05, 1.0, and 5.0 μmol phospholipid·kg$^{-1}$, PM2000 concentration in blood equals to 0.12-, 2.4-, and 12.1-fold of CMC2000 respectively. Data are shown as means ± standard, $n = 3$



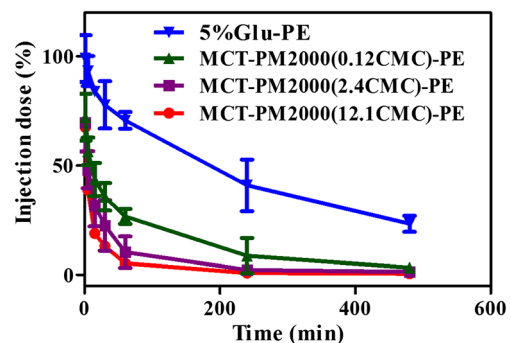**Fig. 6** The effects of lipid dose of MCT-PM2000 on the ABC phenomenon in rats. The rats were pretreated with MCT-PM2000 (0.05, 1.0, and 5.0 μmol phospholipid·kg$^{-1}$) respectively and 7 days later, each group was intravenously injected with 5 μmol phospholipid·kg$^{-1}$ of PE. In addition, after intravenous injection of MCT-PM2000 into circulation at doses of 0.05, 1.0, and 5.0 μmol phospholipid·kg$^{-1}$, MCT-PM2000 concentrations in blood equal to 0.12-, 2.4-, and 12.1-fold of the CMC respectively. Data are shown as means ± standard, $n = 3$
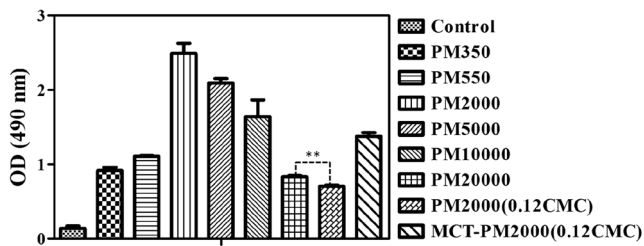
**Fig. 7** Anti-PEG IgM production induced by 5 μmol phospholipid·kg$^{-1}$ of PMy ($y$ = 350, 550, 2000, 5000, 10,000, and 20,000), 0.05 μmol phospholipid·kg$^{-1}$ of PM2000 and 0.05 μmol phospholipid·kg$^{-1}$ of MCT-PM2000 through intravenous injection. Data are shown as means ± standard, $n$ = 3. Significant differences: **$p < 0.05$

result, precipitate was also found in the PM10000 and PM20000 groups. In each group, an equilibrium state can be reached, which requires the lowest system energy. However, PM2000 and PM5000 possess better storage stability than PM350, PM550, PM10000, and PM20000.

When we set the size of PM350, PM550, PM2000, PM5000, PM10000, and PM20000 to be 20 nm manually, the *Zeta* potentials of these micelles decrease; a large difference in *Zeta* values between PM2000 (− 49.00 ± 2.36) and PM10000 (− 14.64 ± 0.77) was also observed. As we know, the negative charge of PM originates from the anionic phosphate groups of DSPE-PEGx ($x$ = 350, 550, 2000, 5000, 10,000, and 20,000). When DSPE-PEGx self-assemble to form micelles, the inner hydrophobic core is composed of DSPEs, and the hydrophilic outer shell is composed of PEGs; PEG chains can shield the inner core. The hydrophilic outer shell of PM10000 is much larger than PM2000, and the negative charge of PM10000 can be better shielded than PM2000. Hence, the *Zeta* value of PM2000 was much lower than that of PM10000. We did not detect any association between storage stability of the PEGylated micelles and their *Zeta* potential values. However, increases in PEG length enhances HLB and CMC values of DSPE-PEGx ($x$ = 350, 550, 2000, 5000, 10,000, and 20,000). Therefore, storage stability of PEGylated micelles is not associated with HLB and CMC values of their unimers.

CMC value is an important parameter for micelles. The dissociation kinetics of micelles diluted below CMC is a topic of much discussion. Based on the principle of entropy, dissociation of micelle clusters should dominate below CMC; however, this process may not be instantaneous and could take minutes to hours, or even days if the dissociation process is kinetically trapped [31]. After diluting PM2000 and MCT-PM2000 to be below CMC2000, we found that the dilution stability of MCT-PM2000 was much better than that of PM2000. Therefore, micelle structures formed by MCT and DSPE-PEG$_{2000}$ are resistant to dissociation, even at extreme dilutions. The combination of MCT and DSPE-PEG$_{2000}$ increases the interfacial tension

between the solvophobic block and the solvent; as the free energy of DSPE-PEG2000 increases, particle dissociation becomes more difficult.

This study revealed that PM2000 and PM5000 induce stronger ABC phenomenon than PM350, PM550, PM10000, and PM20000. Furthermore, the ABC phenomenon induced by MCT-PM2000 is stronger than that induced by PM2000. As discussed above, PM2000 and PM5000 exhibit stronger storage stability than PM350, PM550, PM10000, and PM20000. MCT-PM2000 possesses stronger dilution stability than PM2000. These results suggested that storage stability and dilution stability are positively correlated, and further enhance the ABC phenomenon induced by PEGylated micelles. The accepted mechanism of the ABC phenomenon is as follows: the first dose of PEGylated nanocarriers, which act as TI-2 antigens [17, 32–34], induce secretion of anti-PEG IgM by B cells located in splenic marginal zone [29, 33, 35]; these antibodies bind to the second dose of PEGylated nanocarriers to activate the complement pathway, which then increase the uptake of opsonized nanoparticles by resident liver macrophages [8, 27, 28, 36–39]. PMs that are more stable in vitro are also more stable in the bloodstream and can circulate for a longer period following intravenous injections. With increased circulation time, PMs have more opportunities to stimulate B cells to produce anti-PEG IgM; PM stability increases the PM circulation time and thus further increases the anti-PEG IgM secretion. We found that PM2000 and PM5000, which have stronger storage stability than PM350, PM550, PM10000, and PM20000, induced greater anti-PEG IgM secretion. Similarly, MCT-PM2000, which exhibited enhanced dilution stability than PM2000, induced greater anti-PEG IgM secretion than PM2000. These results revealed a positive correlation between particle stability and anti-PEG IgM secretion level. Furthermore, although the levels of anti-PEG IgM induced by PM20000 (5 μmol phospholipid·kg$^{-1}$) and PM2000 (0.05 μmol phospholipid·kg$^{-1}$, 0.12CMC2000) were comparable, the ABC phenomenon induced by PM2000 at a dose of 0.05 μmol phospholipid·kg$^{-1}$ was much larger than that induced by PM20000. It is possible that PM2000 shows stronger affinity to anti-PEG IgM than PM20000.

Furthermore, we found that the ABC phenomenon can be induced by PM2000, which is stable for only 80 min in the circulation (0.05 μmol phospholipid·kg$^{-1}$); 80 min after injection, PM2000 dissociated into single molecules. In addition, ABC phenomenon was unable to be induced by the DSPE-PEG2000 molecule. It was hypothesized that following a brief interaction between PM2000 and B cells located in splenic marginal zone, B cells can be stimulated to secret anti-PEG IgM. Therefore, caution should be exercised when treating patients with even low concentration of micelles or when combining micelles with other PEGylated formulations.

74

Drug Deliv. and Transl. Res. (2019) 9:66–75

# Conclusion

In this study, we showed that PM2000 and PM5000, which possess greater storage stability than PM350, PM550, PM10000, and PM20000, can induce the strongest ABC phenomenon. MCT-PM2000 showed stronger dilution stability than PM2000, and accordingly, the ABC phenomenon induced by MCT-PM2000 was stronger than that induced by PM2000. Based on our findings, it can be concluded that susceptibility to the ABC phenomenon is positively correlated with stability of PEGylated micelles. In addition, the ABC phenomenon induced by PEGylated micelles can be influenced by PEG chain length and lipid injection dose. These results provide valuable guidance for designing PEGylated micelle formulations in multiple drug therapy.

## Compliance with ethical standards

All institutional and national guidelines for the care and use of laboratory animals were followed.

**Conflict of interest** The authors declare that they have no conflicts of interest.

# References

1. Dams ET, Laverman P, Oyen WJ, Storm G, Scherphof GL, van der Meer JW, et al. Accelerated blood clearance and altered biodistribution of repeated injections of sterically stabilized liposomes. J Pharmacol Exp Ther. 2000;292(3):1071–9.
2. Ishida T, Maeda R, Ichihara M, Mukai Y, Motoki Y, Manabe Y, et al. The accelerated clearance on repeated injection of pegylated liposomes in rats: laboratory and histopathological study. Cell Mol Biol Lett. 2002;7(2):286.
3. Zhao Y, Wang L, Yan M, Ma Y, Zang G, She Z, et al. Repeated injection of PEGylated solid lipid nanoparticles induces accelerated blood clearance in mice and beagles. Int J Nanomedicine. 2012;7:2891–900.
4. Saadati R, Dadashzadeh S, Abbasian Z, Soleimanjahi H. Accelerated blood clearance of PEGylated PLGA nanoparticles following repeated injections: effects of polymer dose, PEG coating, and encapsulated anticancer drug. Pharm Res. 2013;30(4):985–95.
5. Wang L, Wang C, Jiao J, Su Y, Cheng X, Huang Z, et al. Tolerance-like innate immunity and spleen injury: a novel discovery via the weekly administrations and consecutive injections of PEGylated emulsions. Int J Nanomedicine. 2014;9:3645–57.
6. Koide H, Asai T, Hatanaka K, Urakami T, Ishii T, Kenjo E, et al. Particle size-dependent triggering of accelerated blood clearance phenomenon. Int J Pharm. 2008;362(1–2):197–200.
7. Mima Y, Hashimoto Y, Shimizu T, Kiwada H, Ishida T. Anti-PEG IgM is a major contributor to the accelerated blood clearance of polyethylene glycol-conjugated protein. Mol Pharm. 2015;12(7):2429–35.
8. Im H-J, England CG, Feng L, Graves SA, Hernandez R, Nickles RJ, et al. Accelerated blood clearance phenomenon reduces the passive targeting of PEGylated nanoparticles in peripheral arterial disease. ACS Appl Mater Interfaces. 2016;8(28):17955–63.
9. Du N, Guo W, Yu Q, Guan S, Guo L, Shen T, et al. Poly (D, L-lactic acid)-block-poly (N-(2-hydroxypropyl) methacrylamide) nanoparticles for overcoming accelerated blood clearance and achieving efficient anti-tumor therapy. Polym Chem. 2016;7(36):5719–29.
10. Gaucher G, Dufresne M-H, Sant VP, Kang N, Maysinger D, Leroux J-C. Block copolymer micelles: preparation, characterization and application in drug delivery. J Control Release. 2005;109(1–3):169–88.
11. Matsumura Y, Hamaguchi T, Ura T, Muro K, Yamada Y, Shimada Y, et al. Phase I clinical trial and pharmacokinetic evaluation of NK911, a micelle-encapsulated doxorubicin. Brit J Cancer. 2004;91(10):1775–81.
12. Matsumura Y. Poly (amino acid) micelle nanocarriers in preclinical and clinical studies. Adv Drug Deliv Rev. 2008;60(8):899–914.
13. Hamaguchi T, Kato K, Yasui H, Morizane C, Ikeda M, Ueno H, et al. A phase I and pharmacokinetic study of NK105, a paclitaxel-incorporating micellar nanoparticle formulation. Brit J Cancer. 2007;97(2):170–6.
14. Shiraishi K, Hamano M, Ma H, Kawano K, Maitani Y, Aoshi T, et al. Hydrophobic blocks of PEG-conjugates play a significant role in the accelerated blood clearance (ABC) phenomenon. J Control Release. 2013;165(3):183–90.
15. Ma H, Shiraishi K, Minowa T, Kawano K, Yokoyama M, Hattori Y, et al. Accelerated blood clearance was not induced for a gadolinium-containing PEG-poly (L-lysine)-based polymeric micelle in mice. Pharm Res. 2010;27(2):296–302.
16. Kaminskas LM, Mcleod VM, Porter CJ, Boyd BJ. Differences in colloidal structure of PEGylated nanomaterials dictate the likelihood of accelerated blood clearance. J Pharm Sci. 2011;100(11):5069–77.
17. Ishida T, Ichikawa T, Ichihara M, Sadzuka Y, Kiwada H. Effect of the physicochemical properties of initially injected liposomes on the clearance of subsequently injected PEGylated liposomes in mice. J Control Release. 2004;95(3):403–12.
18. Ishida T, Harada M, Wang XY, Ichihara M, Irimura K, Kiwada H. Accelerated blood clearance of PEGylated liposomes following preceding liposome injection: effects of lipid dose and PEG surface-density and chain length of the first-dose liposomes. J Control Release. 2005;105(3):305–17.
19. Zhao Y, Wang C, Wang L, Yang Q, Tang W, She Z, et al. A frustrating problem: accelerated blood clearance of PEGylated solid lipid nanoparticles following subcutaneous injection in rats. Eur J Pharm Biopharm. 2012;81(3):506–13.
20. Perrier T, Saulnier P, Fouchet F, Lautram N, Benoît J-P. Post-insertion into lipid nanocapsules (LNCs): from experimental aspects to mechanisms. Int J Pharm. 2010;396(1–2):204–9.
21. Sezgin Z, Yüksel N, Baykara T. Preparation and characterization of polymeric micelles for solubilization of poorly soluble anticancer drugs. Eur J Pharm Biopharm. 2006;64(3):261–8.
22. Wang C, Cheng X, Su Y, Pei Y, Song Y, Jiao J, et al. Accelerated blood clearance phenomenon upon cross-administration of PEGylated nanocarriers in beagle dogs. Int J Nanomedicine. 2015;10:3533–45.
23. Su Y, Wang L, Liang K, Liu M, Liu X, Song Y, et al. The accelerated blood clearance phenomenon of PEGylated nanoemulsion upon cross administration with nanoemulsions modified with polyglycerin. Asian J Pharm Sci. 2018;13:44–53.
24. Kim SY, Shin IG, Lee YM, Cho CS, Sung YK. Methoxy poly (ethylene glycol) and ε-caprolactone amphiphilic block copolymeric micelle containing indomethacin.: II Micelle formation and drug release behaviours. J Control Release. 1998;51(1):13–22.
25. Liang K, Wang L, Su Y, Liu M, Feng R, Song Y, et al. Comparison among different "revealers" in the study of accelerated blood clearance phenomenon. Eur J Pharm Sci. 2018;114:210–6.

26. Sen S, Sukul D, Dutta P, Bhattacharyya K. Solvation dynamics in aqueous polymer solution and in polymer−surfactant aggregate. J Phys Chem B. 2002;106(15):3763–9.

27. Ishida T, Ichihara M, Wang X, Yamamoto K, Kimura J, Majima E, et al. Injection of PEGylated liposomes in rats elicits PEG-specific IgM, which is responsible for rapid elimination of a second dose of PEGylated liposomes. J Control Release. 2006;112(1):15–25.

28. Ishida T, Wang X, Shimizu T, Nawata K, Kiwada H. PEGylated liposomes elicit an anti-PEG IgM response in a T cell-independent manner. J Control Release. 2007;122(3):349–55.

29. Ishida T, Ichihara M, Wang X, Kiwada H. Spleen plays an important role in the induction of accelerated blood clearance of PEGylated liposomes. J Control Release. 2006;115(3):243–50.

30. Nicolai T, Colombani O, Chassenieux C. Dynamic polymeric micelles versus frozen nanoparticles formed by block copolymers. Soft Matter. 2010;6(14):3111–8.

31. Bae YH, Yin H. Stability issues of polymeric micelles. J Control Release. 2008;131(1):2–4.

32. Semple SC, Harasym TO, Clow KA, Ansell SM, Klimuk SK, Hope MJ. Immunogenicity and rapid blood clearance of liposomes containing polyethylene glycol-lipid conjugates and nucleic acid. J Pharmacol Exp Ther. 2005;312(3):1020–6.

33. Shimizu T, Ishida T, Kiwada H. Transport of PEGylated liposomes from the splenic marginal zone to the follicle in the induction phase of the accelerated blood clearance phenomenon. Immunobiology. 2013;218(5):725–32.

34. Ishida T, Atobe K, Wang X, Kiwada H. Accelerated blood clearance of PEGylated liposomes upon repeated injections: effect of doxorubicin-encapsulation and high-dose first injection. J Control Release. 2006;115(3):251–8.

35. Kim CJ, Hara E, Shimizu A, Sugai M, Kimura S. Activation of B1a cells in peritoneal cavity by T cell-independent antigen expressed on polymeric micelle. J Pharm Sci. 2015;104(5):1839–47.

36. Kaminskas LM, Mcleod VM, Porter H, Christopher J, Boyd BJ. Differences in colloidal structure of PEGylated nanomaterials dictate the likelihood of accelerated blood clearance. J Pharm Sci. 2011;100(11):5069–77.

37. Hashimoto Y, Shimizu T, Lila ASA, Ishida T, Kiwada H. Relationship between the concentration of anti-polyethylene glycol (PEG) immunoglobulin M (IgM) and the intensity of the accelerated blood clearance (ABC) phenomenon against PEGylated liposomes in mice. Biol Pharm Bull. 2015;38(3):417–24.

38. Ishida T, Kashima S, Kiwada H. The contribution of phagocytic activity of liver macrophages to the accelerated blood clearance (ABC) phenomenon of PEGylated liposomes in rats. J Control Release. 2008;126(2):162–5.

39. Hara E, Ueda M, Makino A, Hara I, Ozeki E, Kimura S. Factors influencing in vivo disposition of polymeric micelles on multiple administrations. ACS Med Chem Lett. 2014;5(8):873–7.